Extraction and Characterizations of Mikania micrantha leaf waste for reinforcement in polymer composites.

Biplab Mohapatra
College of Engineering Bhubaneswar, Biju patnaik University of Technology, Odisha

ABSTRACT
Because invasive plants can spread quickly and proliferate, it is commercially feasible to use them to produce goods with added value. In this study, lignocellulosic fiber was recovered via a mercerization technique from the leaf waste of Mikania micrantha Kunth-ex H.B.K., an invasive luxuriant plant. Because a significant portion of the extractive impurities were removed following the alkaline treatment, the lignocellulosic biomass stayed at 38.54%. The mercerized leaf fiber's lignocellulosic fraction increased from 56.59% to 83.96%. The cellulose fraction grew by 11.17%, according to the chemical composition study, while the hemicellulose and lignin fractions fell by 4.89% and 6.28%, respectively. The lignocellulosic fiber's altered chemical composition was further confirmed by the TGA and FT-IR data. Furthermore, the fiber crystallinity index increased from 11.0% to 36.7% with an increase in the cellulose content. The SEM analysis demonstrated that the lignocellulosic fiber's surface shape changed from smooth to rough corrugated ridges, confirming the rise in crystallinity that came about as a result of the wrapped cementing ingredients being removed. The lignocellulosic fiber then demonstrated a greater resistance to water attack, increasing its moisture absorption from 119.22% to 410.19%.

Keywords: Mikania micrantha leaf, Surface modification, mechanical properties, SEM

Introduction

The general consensus is that invasive plant species that flourish in agricultural farmland and native forests should be avoided since they may have a negative influence on agricultural crop productivity, biodiversity, and native plant richness. Specifically, Mikania micrantha, also known as the bittervine, is a "mile-a-minute" creeping climber with freely rapid propagation and a rampant growth habit through its vines (Rai, Sandilya, and Subedi 2012). Because of its dense cover that blocks light, it can disturb, smother, and even destroy nearby plants (Holm et al. 1977). This exotic plant is extensively discarded by using cultural, biological, chemical and mechanical methods, in order to rehabilitate native plant species and to reduce crop yield losses (Flory and Clay 2009; Rai, Sandilya, and Subedi 2012). On the contrary, the invasive plant could provide an abundant source of lignocellulosic fiber, and bioprospection of the plant may unveil its value and profitability.

According to Santana-Meridas, Gonzalez-Coloma, and Sanchez-Vioque (2012), lignocellulosic fibers are thought to be physiologically inert, inexpensive, light weight, renewable, biodegradable, highly tenacious, and easily accessible materials that can be effectively utilized to produce high-value goods. Plant lignocellulosic fibers have a noticeable hygroscopic activity and high moisture absorption when hydrophilic hydroxyl groups are present (Célino et al. 2014). The smart utilization of natural fibers including plant leaf, bast, stalk, fruit, and husk residues rich in lignocellulose content are of great endeavor toward valorization of the agro-wastes (Daud et al. 2014). For instance, jute (*Corchorus spp*.) fiber for the production of geotextiles (Ranganathan 1994) and extracellular polysaccharide (Chowdhury et al. 2012), century (*Agave Americana*) leaf fiber for fabrication of carpets and bioplastics (Hulle, Kadole, and Katkar 2015), sisal (*Agave sisalana*) leaf fiber for manufacturing twines, ropes and dartboards (Dube and Chiyaka 2010), kenaf (*Hibiscus cannabinus* L.) fiber for water softening, absorbent products and automobile (Gharehchahi et al. 2014), hemp (*Cannabis sativa* L.) fiber for producing paper pulps, reinforcement in concrete and biocomposite materials for insulation (Salentijn et al. 2015), flax (*Linum usitatissimum*) fiber for use as implantable materials in surgical meshes (Michel et al. 2014), okra (*Abelmoschus esculentus* L.) fiber for making paper and textiles (Kumar et al. 2013), abaca (*Musa textilis*) leaf fiber for producing meat casings, cordage and tea bags (Vijayalakshmi et al. 2014), ramie (*Boehmeria nivea* L.) fiber for making sacks, carpets and fishing nets (Jose, Rajna, and Ghosh

2017), piassava (*Attalea funifera*) fiber for preparing activated carbon and making brushes, brooms and kiosk roofing (Avelar et al. 2010), sugarcane bagasse (*Saccharum spp*.) stalk fibers for soil matrix and cement composites (Danso et al. 2015), pineapple (*Ananas comosus*) leaf fiber in making threads for textile fabrics (Asim et al. 2015) and reducing sugar (Banerjee et al. 2017), mango (*Mangifera indica*) leaf fiber for bioethanol production (Tarrsini et al. 2018), coir (*Cocos nucifera* L) husk fiber for reinforcing building insulation and cement boards (Verma et al. 2013), cotton (*Gossypium spp*.) stalk fibers for paper, industrial fuel and rayon (Reddy and Yang 2009), citrus (*Citrus sinensis*) peel fibers in food applications such in baked and dairy products, sauces and meats (Lundberg et al. 2014), betel nut (*Piper betle* L.) leaf fiber could serve as a natural filler for polymer composites (Khan et al. 2012) and the neem (*Azadirachta indica*) leaf powder in the alginate beads for the pesticide controlled release formulations (Singh et al. 2010).

The goal of plant waste valorization was achieved by removing lignocellulosic fiber from the leaves of Mikania micrantha, an invasive plant, and characterizing its physicochemical characteristics and chemical composition.

Materials and methods

Materials

The reagents and chemicals were of analytical grade were purchased as follows: methanol (J.T. Baker, USA), glacial acetic acid, sodium hydroxide (Systerm, UN), potassium hydroxide, sodium perchlorite monohydrate (Merck, Germany), and sulfuric acid (R&M Chemicals, UK).

Preparation of lignocellulosic fiber from the leaf waste

A luxuriantly localized invasive plant, *M. micrantha*, at vegetative stage was collected at random from heavily colonized region in the campus of Universiti Putra Malaysia. Initially, the leaves were detached and were naturally dried in an open-air area for a week. The air-dried leaves were pulverized in a grinder, sifted through a 50-mesh sieve and the fine leaf powder was collected. A 100 g of the leaf powder was plunged into conical flasks, which filled with 1 L of methanol. The submerged plant powder was gently stirred using a steel rod for 10 min and left for 3 days at room temperature. Afterwards, the supernatant solution was decanted by passing it through two Whatman filter papers no.1 using a Buchner funnel. The macerated powder residue was collected and was soaked again with methanol using the same method. The extracted crude fiber was dried in a fume hood for an overnight.

Thereafter, the crude fiber powder underwent chemical treatment referring the mercerization methods as reported by (Ray et al. 2001; Sreekala et al. 2000). The crude fiber powder with solid to liquor ratio at 1:50 (w/v) was dipped in the 10% NaOH solution, with applied stirring rate 300 rpm using digital overhead stirrers IKA RW20® (IKA, USA) equipped with a four-blade stainless steel impellers (shaft diameter = 8 mm, shaft length = 350 mm, vane diameter = 50 mm, blade = 50 mm) for 3 h and at room temperature. After the alkaline mercerizing, the supernatant was decanted with the extracted lignocellulosic fiber filtered through a stainless steel sieve. The lignocellulosic fiber was extensively washed with a copious amount of running tap water unceasingly and was rubbed on the sieve, to discard the NaOH residue. Subsequently, the lignocellulosic fiber was scoured thoroughly with distilled water until the pH value reached 7.0. The mercerized fiber was filtered and air dried at room temperature for 48 h and followed by hot air circulating oven drying at 70°C. Prior to the analysis, the extracted lignocellulosic fiber was dried in oven at 105°C. A nontreated sample of the crude fiber was used as a control for comparison.

Determination of the fiber chemical constituents

The chemical compositions of the mercerized lignocellulosic and crude fibers in terms of the % cellulose, hemicellulose, lignin, and ash content were determined in accordance with the standard methods as follows:

(i) Determination of α-cellulose and hemicellulose contents: Five grams of the fiber samples were immersed into the 100 mL of 5% $NaClO_2$ solution, adjusted to pH 4 with drops of

H_2SO_4 and heated at 90°C for 90 min. The resulting holocellulose was filtered through Buchner funnel, washed thoroughly with distilled water, dried in oven at 105°C and cooled down in a desiccator until achieved the constant weight. Thereafter, the holocellulose was mixed with 6% KOH solution and was allowed to stand for 24 h at room temperature. The resulting cellulose was filtered and rinsed with 2% CH_3COOH solution and subsequently washed with distilled water. The cellulose was dried in oven at 105°C, cooled down in desiccator until to achieve constant weight. The hemicellulose fraction was calculated as the difference between the holocellulose and α-cellulose content (Khan et al. 2012).

(ii) Determination of lignin content: One gram of the fiber samples was treated with 20 mL of 72% H_2SO_4 solution and was heated at 110°C for 5 h, in order to hydrolyze the cellulose and hemicellulose. The resulting insoluble residues were extensively washed with hot water, filtered through Buchner funnel and repeatedly rinsed with distilled water until becoming acid free (pH = 7.0). The collected samples were oven dried at 105°C until constant weight (Ververis et al. 2007).

(iii) Determination of ash content: The ash content of the fibers was determined using furnace incineration technique. The samples together with the crucible were dried at 105°C in an oven overnight and were preweighed. Initially, the samples in the crucible were charred on a hot plate and then incinerated at 600°C for 5 h in a muffle furnace. Thereafter, the ash

(iv) residues with the crucible were cooled down in the desiccator and the ash content was gravimetrically quantitated (AOAC 2000). The percent contents of the samples were determined with three replications and the average was reported with standard deviation.

Determination of the fiber chemical functional groups

The chemical characteristics, functional group and peak intensity changes of the fiber samples were determined by using a Spectrum 100 Series FT-IR spectrometer (Perkin Elmer, USA) equipped with an attenuated total reflectance (ATR) sampling device. Samples were positioned on the ATR crystal, and subsequently pressed with a flattip plunger. The IR spectra were analyzed in transmittance mode was scanned within the range of wavenumber of 400–3600 cm^{-1} region, with accumulation of 16 scans per sample, at a scan speed of 0.20 cms^{-1} with a resolution of 4 cm^{-1} and at room temperature.

Determination of the fiber thermal profile

The thermal stability of the chemical composition in the fibers was determined by thermogravimetric analysis (TGA) and differential thermogravimetry (DTG) using a Perkin-Elmer Pyris 7 thermogravimetric analyzer (Perkin Elmer, USA). About 10 mg of samples were placed in platinum pans and heated swept from 50°C to 1000°C with a heating rate of 10°C/min under dynamic flow of nitrogen gas. The weight loss thermograms of the samples as a function of temperature were analyzed using the STAR^e SW 12.10 software (Mettler, Switzerland).

Determination of the fiber crystallinity

Lignocellulosic fiber has a portion of crystalline oriented zones which gives the fiber a certain degree of crystallinity. The alterations of diffraction patterns and degree of crystallinity profiles of the samples were determined by using a Shimadzu XRD 6000 X-ray diffractometer (Shimadzu, Japan) equipped with a diffracted-beam monochromator and a nickel-filtered Cu-Kα target (1.5406 Å) radiation source operating at voltage of 45 kV and at current of 40 mA. The samples were scanned in the diffraction angle (2θ) varying in the range of 10°–30° with scanning rate of 2°/min at room temperature. Thereafter, the samples crystallinity index (I_c %) was calculated by using the Equation (1) (Segal et al. 1959):

$$I_c\% = (I_{002} - I_{am})/I_{002} \times 100 \quad (1)$$

where I_{002} is the maximum intensity of the (0 0 2) lattice diffraction peak at a 2θ between 22° to 23° and I_{am} is the intensity scattered by the (101) amorphous portion of the diffractograms which at a 2θ between 15° and 18°.

Determination of fiber surface morphology

The external morphologies of the transverse and fracture fiber samples were examined using JEOL JSM-6400 scanning electron microscope (SEM) (JEOL Japan) and JEOL JSM-7600F field emission scanning electron microscope (FESEM) (JEOL, Japan), respectively, operating at accelerating voltage of 2–15 kV. Initially, the samples were loaded on the double-sided carbon adhesive tapes, which secured on aluminum stubs holder. The sample surface was sputter-coated with a thin layer of gold by means of a sputter coater unit (E5100 Polaron, UK) under vacuum chamber, to make the samples electrically conductive for generating better image resolution. The photomicrographs of the samples were captured at different magnification.

Determination of water absorption capacity of the fibers

Water absorption capacity of the fiber samples was performed in accordance with the standard procedure described in the ASTM D570 procedure (ASTM 1998). The samples were dried in oven at 105°C, cooled and weighed, until the fiber weight to reach constant. One gram of the samples was immersed into 200 mL distilled water at 25°C for 24 h. The fiber samples were collected from the bulk water through Buchner funnel and patted dried on filter papers to discard the surface water. The percentage of water gain (%W) of the fiber samples was expressed by the Equation (2):

$$\%W = (W_2 - W_1)/W_1 \times 100 \quad (2)$$

where W_1 is the constant dry weight of samples before immersion and W_2 is the wet weight of the samples after immersion. Three replications were done for the moisture gain measurements and were reported in average ± standard error.

Results and discussion

Lignocellulosic fiber study

The crude fiber obtained from leaves of *M. micrantha* was revamped using mercerization process to improve the lignocellulosic content by removal of extractive impurities from the crude sample. Figure 1 shows the resulting sticky agglomerated crude fiber and friable fine mercerized fiber.

Fiber chemical compositions

The chemical compositions of crude and mercerized fibers are summarized in Table 1. The fiber biomass loss incurred resulting from mercerization was 61.46%. A large reduction in the weight fraction of extractive impurities and moisture by 29.01% was observed. No significant change in the ash content with a difference of 1.64%. Aside from that, the chemical composition analysis revealed the lignocellulosic composition with an increase in cellulose fraction by 11.17%. In opposition, reductions in hemicellulose and lignin fractions were found to be 4.89%–6.28%, respectively. The result signifies that the mercerization process induced an increase in the cellulose composition by partial removal of hemicellulose and lignin. The alkaline treatment of sodium hydroxide could prompt hydrolysis of hemicellulose and depolymerization of lignin (Reddy et al. 2016).

(a) (b)

Figure 1. Photographs depict the physical appearances of (a) glutinous aggregated crude fiber (UML) and (b) brittle fine mercerized fiber (MML).

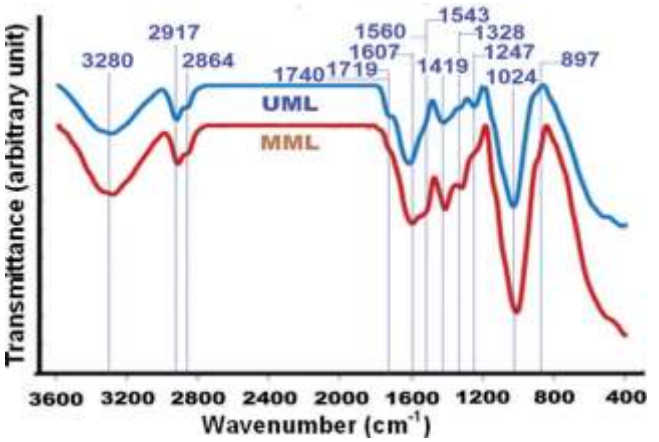

Figure 2. FT-IR spectra of crude fiber (UML) and mercerized fiber (MML).

Fiber chemical functional groups

The chemical groups of cellulose, hemicellulose, and lignin, and the lignocellulosic composition changes in the fibers resulting from the mercerization are presented in the FTIR spectra (Figure 2). It can be noted that the broad intense absorption peak at 3280 cm^{-1} can be assigned to –OH stretching vibration of cellulose and hemicellulose. The symmetric and asymmetric stretching bands at 2917 cm^{-1} and 2864 cm^{-1} correspond to methyl and methylene groups of cellulose and hemicellulose. The absorption peaks at 1740 cm^{-1} and 1719 cm^{-1} belong to carboxyl C = O stretching groups which arose from acetyl groups of hemicellulose and carbonyl aldehyde groups of lignin. Almost disappeared of this peak shoulder after mercerization indicated the minor reductions in hemicellulose and lignin contents, in congruent with the results reported in the chemical composition analysis. An absorption peak at 1607 cm^{-1} can be assigned to –OH bending vibration of the absorbed water inside the fibers. Two absorption bands at 1560 cm^{-1} and 1543 cm^{-1} correspond to conjugated C-O group in the aromatic skeletal and in-plane C = C aromatic ring of lignin. The C-H deformations in methyl, methylene, and methoxyl groups of lignin were observed at 1419 cm^{-1}.

In addition, the absorption peak at 1328 cm^{-1} correlates the N-O stretching vibrations of lignin. These absorption peaks of C-O, C = C, C-H, and N-O groups of lignin became more obvious after mercerization, due to large removal of the extractive impurities. The C-O vibrations of acetyl group in hemicellulose and aryl group in lignin show a stretching band at 1247 cm^{-1}. The almost disappeared of this small peak of the mercerized fiber provided the irrefutable evidence of the partial removal of hemicellulose and lignin. The characteristic C-O vibration at 1024 cm^{-1} belongs to the pyranose ring vibration of cellulose. The peak intensity of C-O vibration of mercerized fiber was observed to be increased in comparison to the crude fiber, signifying an increase in fiber crystallinity (Elanthikkal et al. 2010). A small peak shoulder at 897 cm^{-1} attributed to the ring vibration of –CH deformation of β-glycosidic linkages in the cellulose (Maheswari et al. 2012). The protrusion of this peak shoulder is ascribed to the increase in cellulose content.

Fiber thermogravimetric profile

Stepwise weight losses of the fiber chemical components resulting from thermal decompositions at different temperatures are presented in TGA and DTG curves (Figure 3(a,b)). At initial stage, the TGA curves show scanty amount of weight losses in the crude and mercerized fibers at temperature close to 100°C. The appearance of small peaks in the DTG curves further confirmed the correspond-

ing weight losses were 3.26% and 3.16%. The weight losses around this temperature are mainly

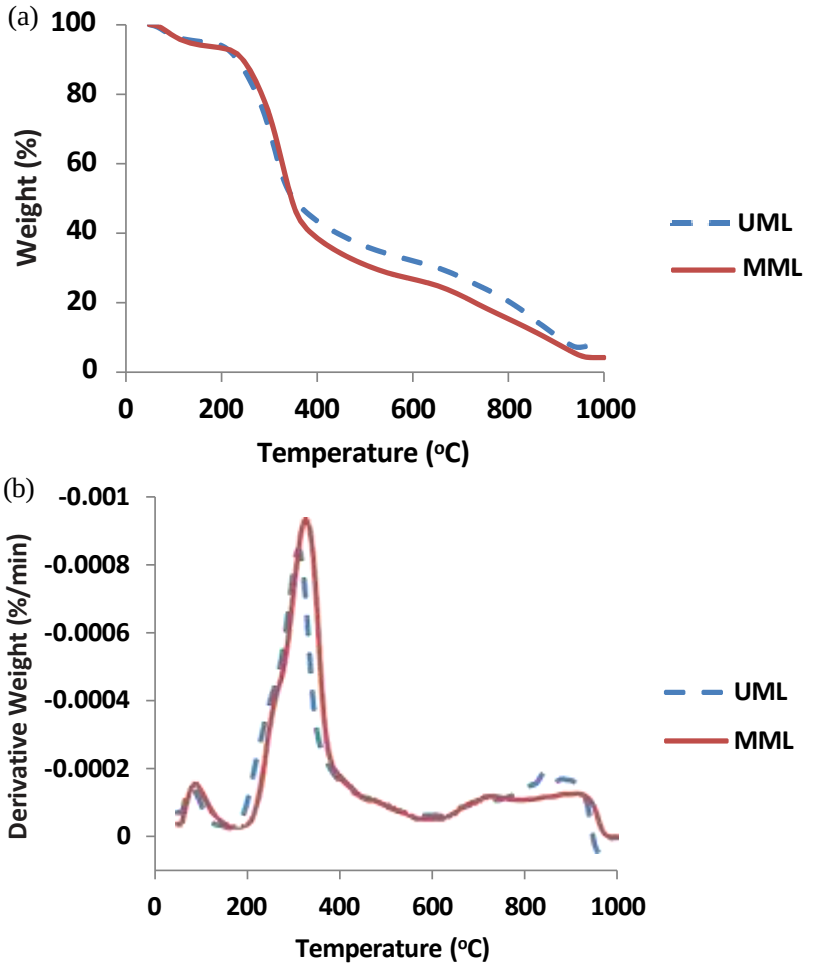

Figure 3. Thermal decompositions of crude (UML) and mercerized (MML) fibers by (a) thermogravimetric analysis and (b) differential thermogravimetry, in the temperature range of 50°C–1000°C. (The highest peaks at UML = 310.85°C and at MML = 326.65°C).

caused by evaporation of physically absorbed water from the fibers (Benini et al. 2016). Further weight decompositions occurred at steep gradient in a temperature ranging from 220°C to 300°C. Thermal decompositions within this temperature range are associated with the degradation of hemicellulose (Reddy et al. 2016). The DTG curves depict the shoulders of the highest peaks correspond to the weight loss in the crude fiber accounted for 22.34%, and this amount was higher than the weight loss in the mercerized fiber which accounted for 18.58%, indicating the meager reduction of hemicellulose content.

Thereafter, the TGA curves show continuing weight reductions at a temperature range of 310°C– 400°C. The salient thermal decomposition of cellulose via cleavage of glycosidic bonds has been reported at a temperature range of 312°C–400°C (Rachini et al. 2009; Reddy et al. 2016). The DTG curves display the weight losses accounted for 27.13% and 36.50% corresponding to the crude and mercerized fibers, confirming higher cellulose content resulting from the mercerization process. At final stage, the TGA curves illustrate the thermal degradations happening in slow rates across a broad temperature range from 420°C to 900°C. The DTG curves depict no sharp peak but rather inconsistent patterns of weight losses. The weight losses in the crude and mercerized fibers were 31.20% and 28.26%,

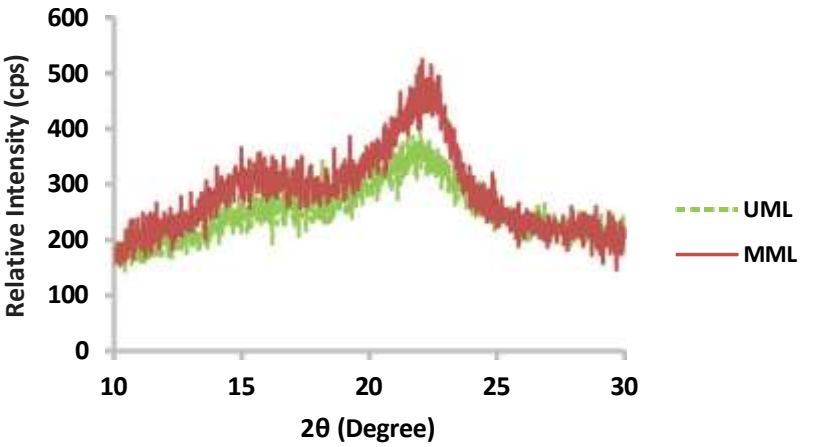

Figure 4. XRD diffractograms of the crude fiber (UML) and the mercerized fiber (MML).

respectively. Thermal degradation of lignin in a significant amount has been reported at the tempera- ture range from 417°C to 816°C (Zainuddin et al. 2014). The meager difference in the lignin fraction between crude and mercerized fiber are represented by the close gap between the two curves in the broad temperature range. At the temperature of 900°C, the weights of char residues of the crude and mercerized fibers remained at 10.54% and 8.35%, respectively.

Fiber crystallinity

The crystallinity behaviors of crude and mercerized fibers are shown in the XRD diffractograms (Figure 4). It can be seen that a broad peak at 2θ values of 15°–16° and a sharp peak at 22°–23° correspond to amorphous and crystalline characteristics of the semi-crystalline fibers. The two diffraction peaks of mercerized fiber exhibit more prominent in higher signal intensity than the crude fiber. As tabulated in Table 2, evidently the mercerization process increased the crystallinity index from 11.0% to 36.7%, proving the higher crystallinity of mercerized fiber. The rise in crystal- linity is associated with the heavy removal of extractive impurities and partial eliminations of hemicellulose and lignin enriching the cellulose fraction. The alkaline treatment can provide the fiber with a more crystalline surface, enhance mechanical strength and cellulose accessibility, and promote extensive binding capability between fiber and matrix (Barakat, de Vries, and Rouau 2013; Reddy et al. 2013).

Fiber surface morphology

SEM micrographs confirmed the fiber surface was modified by alkaline etching treatment, as portrayed in Figure 5. Before treatment, the fiber surface was noted to be smooth and wrapped by cementing materials. After mercerization, the fiber surface exhibited a pronounced exposure of fibrils as aligned corrugated ridges in closely packed arrangement. The rearranged closer and highly organized internal fibrils could impart higher crystallinity (Banerjee et al. 2017). The alkaline treatment was found to effectively liberate the fiber surfaces from the binding impurities with increased surface roughness of the interfibrillar region. The rough surface of fiber bundles produced

Table 2. Crystallinity index of the unmodified and mercerized fibers.

Fiber	I_{am} (cps)	I_{002} (cps)	I_c %
[a]UML	356(15.72 °)	400(22.00 °)	11.0
[b]MML	300(15.98 °)	474(22.48 °)	36.7

[a]UML – unmodified crude fiber; [b]MML – mercerized fiber.

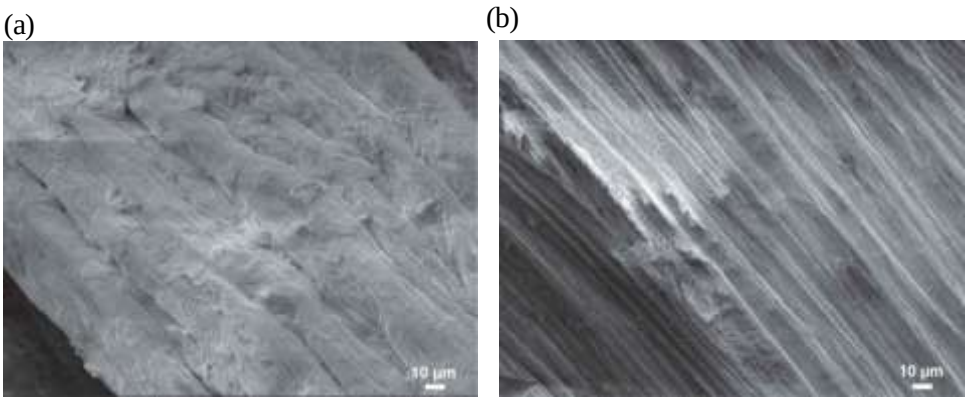

Figure 5. SEM micrographs of (a) crude fiber (UML) with smooth surface and (b) mercerized fiber (MML) with surface etching.

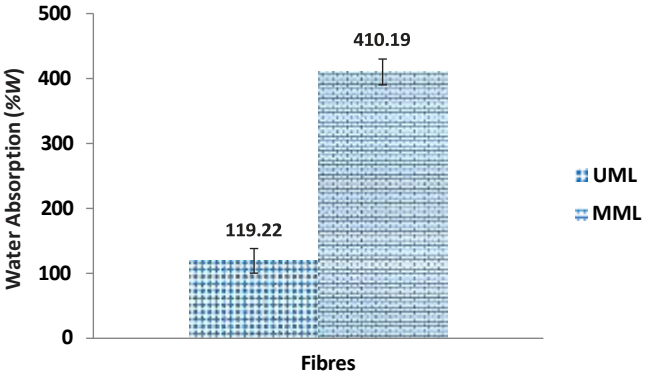

Figure 6. Water absorption capacity of the crude (UML) and mercerized (MML) fibers.

by alkaline treatment have been reported after the removal of waxy coating of cuticles (Hujuri et al. 2008), hemicellulose and lignin (Oushabi et al. 2017; Reddy et al. 2014). The surface etching treatment could enhance fiber-matrix interfacial adhesion and interlocking (Kalia et al. 2011; Moreira and Seo 2016).

Fiber water absorption

The water absorption profiles of crude and mercerized fibers are shown in Figure 6. The crude fiber exhibited absorption of 110% water content, which was more than its weight. Generally, the raw natural fiber could absorb 100% to 200% of water content by weight at room temperature (Célino et al. 2013). In opposition, the moisture content of mercerized fiber was found to be increased strikingly with about 3.5-fold higher than the moisture content in the crude fiber, indicating the mercerized fiber surface was more pervious to water absorption. The increase in water absorption capacity can be principally accredited to the removal of extractive impurities, which allow the fiber surface greater exposure of hydroxyl groups of cellulose and hemicellulose for more water accessibility via hydrogen bonding. Mercerization enhances the fiber with more reactive sites and improved fiber wetting (Kalia et al. 2011). The water absorption prefers the amorphous site of the cellulose in the fiber (Célino et al. 2013; Reddy et al. 2009).

Conclusions

Overall, mercerization process purified the crude fiber with generating higher composition of lignocellulosic content. This alkali treatment removed the cementing extractive impurities and reduced minor fractions of the hemicellulose and lignin, thus resulting in an increase in cellulose fraction, as evidenced by the chemical composition analysis, FT-IR and TGA. As a result, the extracted lignocellulosic fiber exhibited higher crystallinity index, rougher surface morphology and improved moisture absorption. This well-characterized alkaline-treated fiber can be used as renew- able lignocellulosic source for coating or composite materials or nanocellulose extraction, in creating value-added products for sustainable agriculture practices, in the aim of reducing agro-wastes.

References

American Standards for Testing and Materials (ASTM), D570. 1998. *Standard test method for water absorption of polymers and plastics, International*. West Conshohocken, PA.

Asim, M., K. Abdan, M. Jawaid, M. Nasir, Z. Dashtizadeh, M. R. Ishak, and M. E. Hoque. 2015. A review on pineapple leaves fibre and its composites. *International Journal of Polymer Science* 950567:1–16. doi:10.1155/2015/950567.

Association of Official Analytical Chemists, AOAC. 2000. *Official methods of analysis*. AOAC International, Washington, DC.

Avelar, F. F., M. L. Bianchi, M. Goncalves, and E. G. Mota. 2010. The use of piassava fibers (*Attalea funifera*) in the preparation of activated carbon. *Bioresource Technology* 101:4639–45. doi:10.1016/j.biortech.2010.01.103.

Banerjee, R., A. D. Chintagunta, and S. Ray. 2017. A cleaner and eco-friendly bioprocess for enhancing reducing sugar production from pineapple leaf waste. *Journal of Cleaner Production* 149:387–95. doi:10.1016/j.jclepro.2017.02.088.

Barakat, A., H. de Vries, and X. Rouau. 2013. Dry fractionation process as an important step in current and future lignocellulose biorefineries: A review. *Bioresource Technology* 134:362–73. doi:10.1016/j.biortech.2013.01.169.

Benini, K. C. C. C., H. J. C. Voorwald, M. O. H. Cioffi, A. C. Milanese, and H. L. Ornaghi. 2016. Characterization of a new lignocellulosic fiber from Brazil: *imperata brasiliensis* (Brazilian Satintail) as an alternative source for nano-cellulose extraction. *Journal of Natural Fibers* 14:112–25. doi:10.1080/15440478.2016.1167647.

Célino, A., S. Freour, F. Jacquemin, and P. Casari. 2014. The hygroscopic behavior of plant fibers: a review. *Frontiers in Chemistry: Polymer Chemistry* 1 (43):1–12. doi:10.3389/fchem.2013.00043.

Célino, A., S. Fréour, F. Jacquemin, and P. Casari. 2013. Characterization and modeling of the moisture diffusion behaviour of natural fibres. *Journal of Applied Polymer Science* 130:297–306. doi:10.1002/app.39148.

Chowdhury, S. R., R. K. Basak, R. Sen, and B. Adhikari. 2012. Utilization of lignocellulosic natural fiber (jute) components during a microbial polymer production. *Materials Letters* 66:216–18. doi:10.1016/j. matlet.2011.08.040.

Danso, H., D. B. Martinson, M. Ali, and J. B. Williams. 2015. Effect of sugarcane bagasse fibre on the strength properties of soil blocks. International Conference on Bio-based Building Materials, Clermont-Ferrand, France, June 22nd-24th.

Daud, Z., M. Zainuri, M. Hatta, A. Sari, M. Kassim, H. Awang, and A. M. Aripin. 2014. Exploring of agro waste (pineapple leaf, corn stalk, and Napier grass) by chemical composition and morphological study. *Bioresources* 9:872–80.

Dube, S., and C. Chiyaka. 2010. Biological and physical features of sisal (agave sp.). *Varieties Growing in Matebeleland Region. Journal Of Biology and Life Sciences* 1:22-26.

Elanthikkal, S., U. Gopalakrishnapanicker, S. Varghese, and J. T. Guthrie. 2010. Cellulose microfibres produced from banana plant wastes: isolation and characterization. *Carbohydrate Polymers* 80 (3):852–59. doi:10.1016/j. carbpol.2009.12.043.

Flory, S. L., and K. Clay. 2009. Invasive plant removal method determines native plant community responses. *Journal of Applied Ecology* 46:434–42. doi:10.1111/jpe.2009.46.issue-2.

Gharehchahi, E., A. H. Mahvi, S. M. T. Shahri, and R. Davani. 2014. Possibility of application of kenaf fibers (*Hibiscus cannabinus* L.) in water hardness reduction. *Desalination and Water Treatment* 52:31–33. doi:10.1080/ 19443994.2013.819137.

Holm, L. G., D. L. Plucknett, J. V. Pancho, and J. P. Herberger. 1977. *The world's worst weeds: distribution and biology*. Honolulu, HI: University Press of Hawaii.

Hujuri, U., S. K. Chattopadhay, R. Uppaluri, and A. K. Ghoshal. 2008. Effect of maleic anhydride grafted polypropy- lene on the mechanical and morphological properties of chemically modified short-pineapple-leaf-fiber-reinforced polypropylene composites. *Journal of Applied Polymer Science* 107 (3):1507–16. doi:10.1002/(ISSN)1097-4628.

Hulle, A., P. Kadole, and P. Katkar. 2015. *Agave Americana* leaf fibers. *Fibers* 3:64–75. doi:10.3390/fib3010064.

Jose, S., S. Rajna, and P. Ghosh. 2017. Ramie fibre processing and value addition. *Asian Journal of Textile* 7 (1):1–9. doi:10.3923/ajt.2017.1.9.

Kalia, S., A. Dufresne, B. M. Cherian, B. S. Kaith, L. Avérous, J. Njuguna, and E. Nassiopoulos. 2011. Cellulose-based bio- and nanocomposites: A review. *International Journal of Polymer*

Science 837875:1–35.

Khan, G. M. A., S. R. S. Palash, M. S. Alam, A. K. Chakraborty, M. A. Gafur, and M. Terano. 2012. Isolation and characterization of betel nut leaf fiber: Its potential application in making composites. *Polymer Composites* 33 (5):764–72. doi:10.1002/pc.v33.5.

Kumar, D. S., D. E. Tony, A. P. Kumar, K. A. Kumar, D. B. S. Rao, and R. Nadendla. 2013. A review on: *Abelmoschus esculentus* (okra). *International Research Journal of Pharmaceutical and Applied Sciences* 3 (4):129–32.

Lundberg, B., X. J. Pan, A. White, H. Chau, and A. Hotchkiss. 2014. Rheology and composition of citrus fiber. *Journal of Food Engineering* 125:97–104. doi:10.1016/j.jfoodeng.2013.10.021.

Maheswari, C. U., K. O. Reddy, E. Muzenda, B. R. Guduri, and A. V. Rajulu. 2012. Extraction and characterization of cellulose microfibrils from agricultural residue-*Cocos nucifera L*. *Biomass and Bioenergy* 46 (12):555–63. doi:10.1016/j.biombioe.2012.06.039.

Michel, S. A., R. R. Vogels, N. D. Bouvy, M. L. Knetsch, N. M. van den Akker, M. J. Gijbels, C. van der Marels, J. Vermeersch, D. G. Molin, and L. H. Koole. 2014. Utilization of flax fibers for biomedical applications. *Journal of Biomedical Materials Research* 102 (3):477–87. doi:10.1002/jbm.b.33025.

Moreira, T. M., and E. S. M. Seo. 2016. Corn leaf fibers preparation and characterization for composite obtention.

Materials Science Forum 881:271–76. doi:10.4028/www.scientific.net/MSF.881.271.

Oushabi, A., S. Sair, F. O. Hassani, Y. Abboud, O. Tanane, and A. El-Bouari. 2017. The effect of alkali treatment on mechanical, morphological and thermal properties of date palm fibers (DPFs): study of the interface of DPF–Polyurethane composite. *South African Journal of Chemical Engineering* 23:116–23. doi:10.1016/j.sajce.2017.04.005.

Rachini, A., M. Le Troedec, C. Peyratout, and A. Smith. 2009. Comparison of the thermal degradation of natural, alkali-treated and silane-treated hemp fibers under air and an inert atmosphere. *Journal of Applied Polymer Science* 112 (1):226–34. doi:10.1002/app.v112:1.

Rai, R. K., M. Sandilya, and R. Subedi. 2012. Controlling *Mikania micrantha* HBK: how effective manual cutting is?

Journal of Ecology and Field Biology 35 (3):235–42.

Ranganathan, S. R. 1994. Development and potential of jute geotextiles. *Geotextiles and Geomembranes* 13 (6–7):421–

33. doi:10.1016/0266-1144(94)90006-X.

Ray, D., B. K. Sarkar, A. K. Rana, and N. R. Bose. 2001. Effect of alkali treated jute fibres on composite properties.

Bulletin of Materials Science 24 (2):129–35. doi:10.1007/BF02710089.

Reddy, K. O., B. Ashok, K. R. N. Reddy, Y. E. Feng, J. Zhang, and A. V. Rajulu. 2014. Extraction and characterization of novel lignocellulosic fibers from *Thespesia Lampas* plant. *International Journal of Polymer Analysis and Characterization* 19 (1):48–61. doi:10.1080/1023666X.2014.854520.

Reddy, K. O., C. U. Maheswari, D. J. P. Reddy, and A. V. Rajulu. 2009. Thermal properties of napier grass fibers.

Materials Letters 63:2390–92. doi:10.1016/j.matlet.2009.08.035.

Reddy, K. O., C. U. Maheswari, E. Muzenda, M. Shukla, and A. V. Rajulu. 2016. Extraction and characterization of cellulose from pretreated *Ficus* (Peepal tree) leaf fibers. *Journal of Natural Fibers* 13:54–64. doi:10.1080/15440478.2014.984055.

Reddy, K. O., C. U. Maheswari, M. Shukla, J. I. Song, and A. V. Rajulu. 2013. Tensile and structural characterization of alkali treated Borassus fruit fine fibers. *Composites Part B: Engineering* 44 (1):433–38. doi:10.1016/j.compositesb.2012.04.075.

Reddy, N., and Y. Q. Yang. 2009. Properties and potential applications of natural cellulose fibers from the bark of cotton stalks. *Bioresource Technology* 100:3563–69. doi:10.1016/j.biortech.2009.02.047.

Salentijn, E. M. J., Q. Y. Zhang, S. Amaducci, M. Yang, and L. M. Trindade. 2015. New developments in fiber hemp (*Cannabis sativa* L.) breeding. *Industrial Crops and Products* 68:32–41. doi:10.1016/j.indcrop.2014.08.011.

Santana-Meridas, O., A. Gonzalez-Coloma, and R. Sanchez-Vioque. 2012. Agricultural residues as a source of bioactive natural products. *Phytochemistry Reviews* 11 (4):447–66. doi:10.1007/s11101-012-9266-0.

Segal, L. G. J. M. A., J. J. Creely, A. E. Martin, and C. M. Conrad. 1959. An empirical method for estimating the degree of crystallinity of native cellulose using the X-ray diffractometer. *Textile Research Journal* 29 (10):786–94. doi:10.1177/004051755902901003.

Singh, B., D. K. Sharma, R. Kumar, and A. Gupta. 2010. Development of a new controlled pesticide delivery system based on neem leaf powder. *Journal of Hazardous Materials* 177:290–99. doi:10.1016/j.jhazmat.2009.12.031.

Sreekala, M. S., M. G. Kumaran, S. Joseph, M. Jacob, and S. Thomas. 2000. Oil palm fibre reinforced phenol formaldehyde composites: Influence of fibre surface modifications on the mechanical performance. *Applied Composite Materials* 7 (5–6):295–329. doi:10.1023/A:1026534006291.

Tarrsini, M., Y. P. Teoh, Q. H. Ng, B. Kunasundari, Z. X. Ooi, H. S. Shuit, and P. Y. Hoo. 2018. Practicability of lignocellulosic waste composite in controlling air pollution from leaves litter through bioethanol production. *IOP Conference Series: Materials Science and Engineering* 318:012001. doi:10.1088/1757-899X/318/1/012001.

Verma, D., P. C. Gope, A. Shandilya, A. Gupta, and M. K. Maheshwari. 2013. Coir fibre

reinforcement and application in polymer composites: A review. *Journal of Materials and Environmental Science* 4 (2):263–76.

Ververis, C., K. Georghiou, D. Danielidis, D. G. Hatzinikolaou, P. Santas, R. Santas, and V. Corleti. 2007. Cellulose, hemicelluloses, lignin and ash content of some organic materials and their suitability for use as paper pulp supplements. *Bioresource Technology* 98:296–301. doi:10.1016/j.biortech.2006.01.007.

Vijayalakshmi, K., C. Y. K. Neeraja, A. Kavitha, and J. Hayavadana. 2014. Abaca fibre. *Transactions on Engineering and Sciences* 2 (9):16–19.

Zainuddin, M. F., R. Shamsudin, M. N. Mokhtar, and D. Ismail. 2014. Physicochemical properties of pineapple plant waste fibers from the leaves and stems of different varieties. *BioResources* 9 (3):5311–24. doi:10.15376/ biores.9.3.5311-5324.